Towards a New Order of the Polyhedral Honeycombs: Part III: The Developed Metaorder, Form and Counterform

Robert C. Meurant

Director Emeritus, Institute of Traditional Studies; Adjunct Professor, Seoul National University College of Engineering PG Dept.; Exec. Director, Research & Education, Harrisco Enco • 4/1108 Shin-Seung Apt, ShinGok-Dong 685 Bungi, Uijeongbu-Si, Gyeonggi-Do, Republic of Korea 480-070 • Email: rmeurant@gmail.com

Abstract

This extended version of a third part of a series of papers applies the metaorder of the all-space-filling periodic polyhedral honeycombs developed by the author to their potential configurations of form and counterform. The individual periodic polyhedral honeycomb can be differentiated into a subset of contiguous periodic polytopes, the *form*, while the remaining space comprises another subset of contiguous periodic polytopes, the *counterform*. Form and Counterform fill all space. While in certain cases, the contiguity of a subset is through just neutral vertex; axial, transverse, or diagonal edge; or diagonal prism, rather than through neutral axial polygon or polyhedron, the behavior is rigorous, and validates the metaorder of these honeycombs that I have previously advanced. As in the well known figure-background perception phenomenon in psychology, form and counterform are interchangeable, depending on which is being attended to. But each demonstrates parallel and consistent structure within each of the three symmetry classes. In each specific case, form and counterform are intertwined with each other, and divide space into two. Form and counterform are identical in four cases; and identical, but enantiomorphic, in another. The expansion sequences of honeycombs in Classes II and III that I have elsewhere identified apply, so within each sequence, its form follows an expansion sequence, whilst its counterform simultaneously follows a corresponding counter-sequence, and these are consistent for each sequence in the class. The investigation into form and counterform provides a platform to apply and validate the metaorder of these all-space-filling periodic polyhedral honeycombs, and suggests further development and potential applications of the geometries.

Keywords: all-space-filling, polyhedra, honeycomb, structural morphology, form, counterform, order.

Supplementary Information: Color graphics can be found at http://www.rmeurant.com/its/si-4.html
Related research by the author can be found at http://www.rmeurant.com/its/papers/polygon-1.html

This paper substantially develops and expands my earlier paper *"Form and Counterform in the All Space-filling Periodic Polyhedral Honeycombs",* in L. Li and C.-C. Hung (eds.), *Proceedings of The Ninth International Conference on Information*, Tokyo, December 7–9, 2018, 51–56 [1].

Glossary

GE : The 4 Great Enablers, of +/– orientation Tetrahedron T^+, T^-, or truncateD tetrahedron, D^+, D^-.

PP : The 8 Primary Polytopes: VerTex VT, CuBe CB, Truncated Octahedron TO, Great Rhomic cuboctahedron GR, OctaHedron OH, CubOctahedron CO, Truncated Cube TC, and Small Rhombic octahedron SR.

NE : The 10 Neutral Elements: the Diagonal Edge DE (i.e., √2), (2D) Neutral Vertex NV, (transverse) Square SQ (elsewhere Neutral Square NS), Rotated Square RS, and OctaGon OG, and their respective prisms, the Diagonal Prism DP (axial square), Axial Edge AE, Square Prism SP (neutral cube), Rotated Prism RP (rotated cube), and Octagonal Prism OP.

RCL : Reference Cubic Lattice, RCL_1 and RCL_2, each with nodes at the centers of the other's cubes.

RTL : Reference Tetrahedral Lattice, there being two for each RCL: RTL_1^{α} and RTL_1^{β}, RTL_2^{α} and RTL_2^{β}.

$V3$: √3 axial Vertex "face" of VT, CB, or T. $V4$: √1 axial Vertex "face" of VT. (+)ve: positive.

TR : √3 axial Triangular face, +ve (upper Δ) TR^+ of OH, SR, or D; –ve (up. ∇) TR^- of TC, CO, or T.

HG : √3 axial Hexagonal face, of TO, GR, or D. TE : √2 axial Transverse Edge. (–)ve: negative.

1. Introduction

In this paper, I apply the metaorder of the all-space-filling periodic polyhedral honeycombs that I have elsewhere advanced [3–6] to the perspective of form and counterform, which together fill all space. Inspired by Keith Critchlow's *Order in Space* [7], my analysis of the polyhedral honeycombs differentiates them into three classes on the basis of the symmetry that the centers of the polytopes of their lattices display, viz. Classes I {2,3,3|2,3,3} (1 kind); II: {2,3,3|2,3,4} (4 distinct kinds); and III: {2,3,4|2,3,4} (10 distinct kinds). The honeycombs are comprised of various combinations of three distinct kinds of polytopes: the two "Great Enablers" $GE = T$ and D in (+/–)-ve orientation (T^+, T^-, D^+, D^-); eight Primary Polytopes PPs: (VT, CB, TO, GR, OH, CO, TC, SR); and the 10 Neutral Elements NEs that mediate them along the √1 XYZ axes. GEs and PPs are situated at nodes of reference cubic lattices RCL_1 and RCL_2; the nodes RC_1 of one lattice are located at the centers of the reference cubes RC_2 of the other lattice. Either RCL can be differentiated into component tetragonal lattices RTL^{α} and RTL^{β}, so RTL_1: RTL_1^{α} of nodes RT_1^{α}, and RTL_1^{β} of RT_1^{β}; and RTL_2: RTL_2^{α} of nodes RT_2^{α}, and RTL_2^{β} of RT_2^{β}. The 3 classes are characterized by different types of alternation, which are determined by which GEs or PPs are situated at which nodes of the RCLs or RTLs.

This analysis differs from previous analyses [7–9] in my differentiation of honeycombs into 3 symmetry classes, elements into GEs, PPs, and NEs, and PPs into self-reflective and not; inclusion of VT as a PP; inclusion of the regular OP as a neutral polyhedron, and extension of neutral elements to include 0D, 1D, and 2D polytopes, as well as 3D polyhedra; recognition of sequences of expansion of the honeycombs in Classes II and III, and clusters thereof in Class III; and the recognition of $[VT_1 \mid CB_2]_{AE_1}^{SQ_2}$ and $[VT_1 \mid VT_2]_{NV_1}^{NV_2}$ as honeycombs.

For convenience of exposition, I consider the classes in reverse order, and commence with Class III, which is characterized by a simple alternation of PP_1 and PP_2 on RCL_1 and RCL_2, though note that both RCLs could be distinguished into their two respective component RTLs, RTL^{α} and RTL^{β}, to constitute an alternation of alternations. Secondly, the Class III honeycombs can be further differentiated into whether they are self-reflective ($PP_1 = PP_2$) (i.e. the same polytope), or not ($PP_1 \neq PP_2$). Fundamental to this differentiation is the apprehension that the various PPs are not equivalent, though they do emerge as different characterizations of the same more profound integral order. In similar fashion, the differentiation of component polytopes into GEs, PPs, and NEs recognizes that not all components are equivalent – they have unique qualities both in terms of sub-class and as individuals, while still revealing a coherent order underlying their patterns of association.

Class II is characterized by an alternation of alternations, as in RCL_1 consisting of an alternation of PP_1 and PP_2, while RCL_2 consists of an alternation of GE^+ and GE^-, where for the one honeycomb, GE is either $T^{+/-}$ or $D^{+/-}$, but cannot be both. The patterns of association of PP_1 and PP_2 reflect in different fashion their differentiation in Class III.

Finally, Class I – which I regard as the most subtle of the honeycombs, and the most difficult to properly appreciate – is characterized by a complex four-way alternation of both plus and minus forms of both GEs, so that $RCL_1 = [RTL_1^{\alpha} = T^+$ and $RTL_1^{\beta} = D^-]$, while $RCL_2 = [RTL_2^{\beta} = D^+$ and $RTL_2^{\beta} = T^-]$, where superscripts +/– denote alternative orientations (of T or D in its reference circum-cube). Neutral Elements (NEs) of {2,2,4} symmetry are located on the respective √1 XYZ axes, so demonstrate one of 3 primary XYZ orientations.

2. The three classes of honeycombs and their constituent sets of polytopes

2.1. Class III

The {2,3,4|2,3,4} Class III honeycombs are constituted of either 1 or 2 PPs and their respective NEs; in the case of 1 PP, this simply means that although there are two PPs, they are the same PP, though they can be considered as being of different color according to their location (they play different roles). So the Class III honeycombs comprise four different two-step expansion/contraction sequences of honeycomb from contracted form through intermediary form to expanded form (Fig. 1 A). These consist of a self-reflective primary sequence (Fig. 1 D), a non-self-reflective secondary sequence (Fig. 1 C) that appears as two enantiomorphs of one another, and a self-reflective tertiary sequence (Fig. 1 B). The steps in each sequence are characterized by in the first step, one set of PPs separating by unit distance, while the other set morphs from one PP to another; and then in the second step, the first set of PPs morphing from one PP to another, while the other (new) set of PPs separates by unit distance. There are only 4 kinds of morphs, and this fundamental behavior of simultaneous separation and morphing extends into Class II, and even to the order relating the polytopes within one symmetry class (which I am in the process of thus revising). (This lattice expansion sequence is well described in the earlier papers [1–6]). So in the various Class III honeycombs, pairs of proximate PPs can either be contiguous (*adjoining*; in the contracted state in the contracted or intermediary forms); or non-contiguous, separated by unit distance (*adjacent*; in the expanded state in the intermediary or expanded forms of the honeycombs). Meanwhile, in the contracted state of PPs, NEs can only have zero extent along their primary X, Y, or Z (XYZ) axis, so are considered to be either neutral vertex (NV), transverse (√1) (TE) or diagonal (√2) (DE) edge, or transverse polygon of neutral square (SQ), rotated square (RS), or octagon (OG). In the expanded state of PPs, these neutral polytopes have been projected along their primary axis (by unit length), to form axial edge (AE), transverse (√1) square SQ or diagonal (√2) prism (DP), or prismatic (neutral) square prism (neutral cube) (SP), rotated square prism (rotated cube) (RP), or (regular) octagonal prism (OP). Note again that each of these neutral polytopes has a primary XYZ axis, and two minor XYZ axes, so they come in three primary orientations. For practical applications, they can each be further differentiated if desired into +ve or –ve forms, according to the direction of their normal along the XYZ axis.

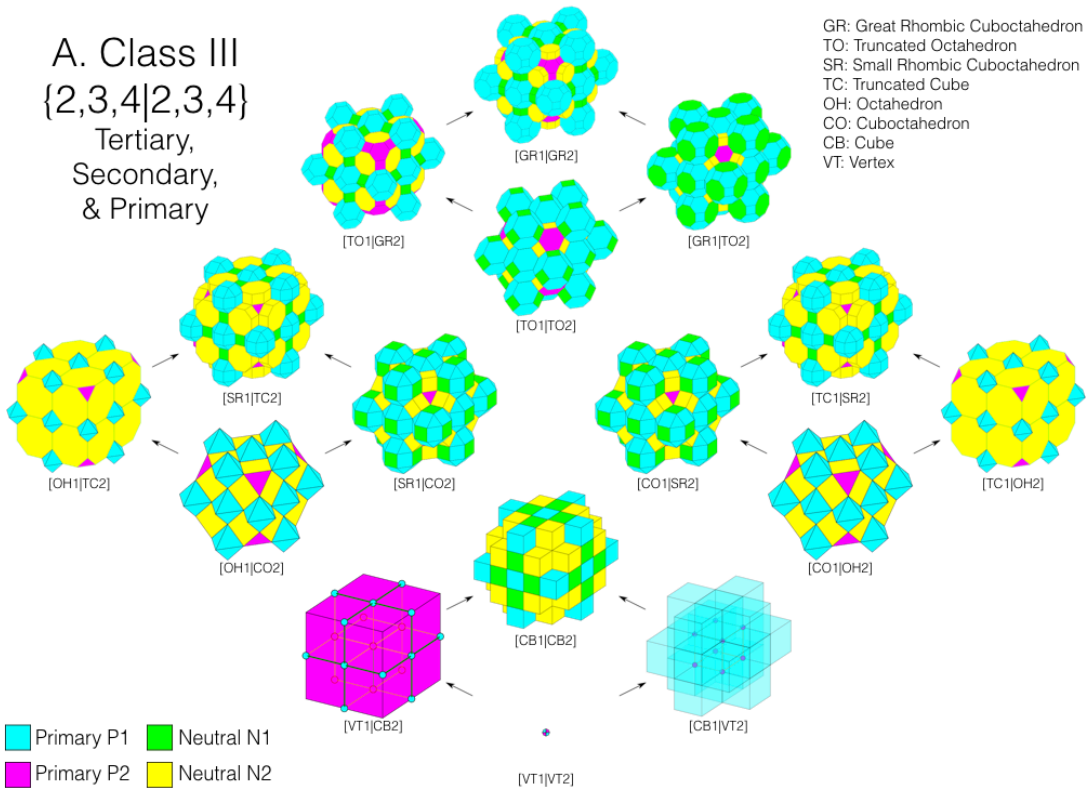
A. Class III
{2,3,4|2,3,4}
Tertiary,
Secondary,
& Primary
GR: Great Rhombic Cuboctahedron
TO: Truncated Octahedron
SR: Small Rhombic Cuboctahedron
TC: Truncated Cube
OH: Octahedron
CO: Cuboctahedron
CB: Cube
VT: Vertex
[GR1|GR2]
[TO1|GR2]
[GR1|TO2]
[TO1|TO2]
[SR1|TC2]
[TC1|SR2]
[OH1|TC2]
[SR1|CO2]
[CO1|SR2]
[TC1|OH2]
[OH1|CO2]
[CO1|OH2]
[CB1|CB2]
[VT1|CB2]
[CB1|VT2]
[VT1|VT2]
Primary P1
Primary P2
Neutral N1
Neutral N2

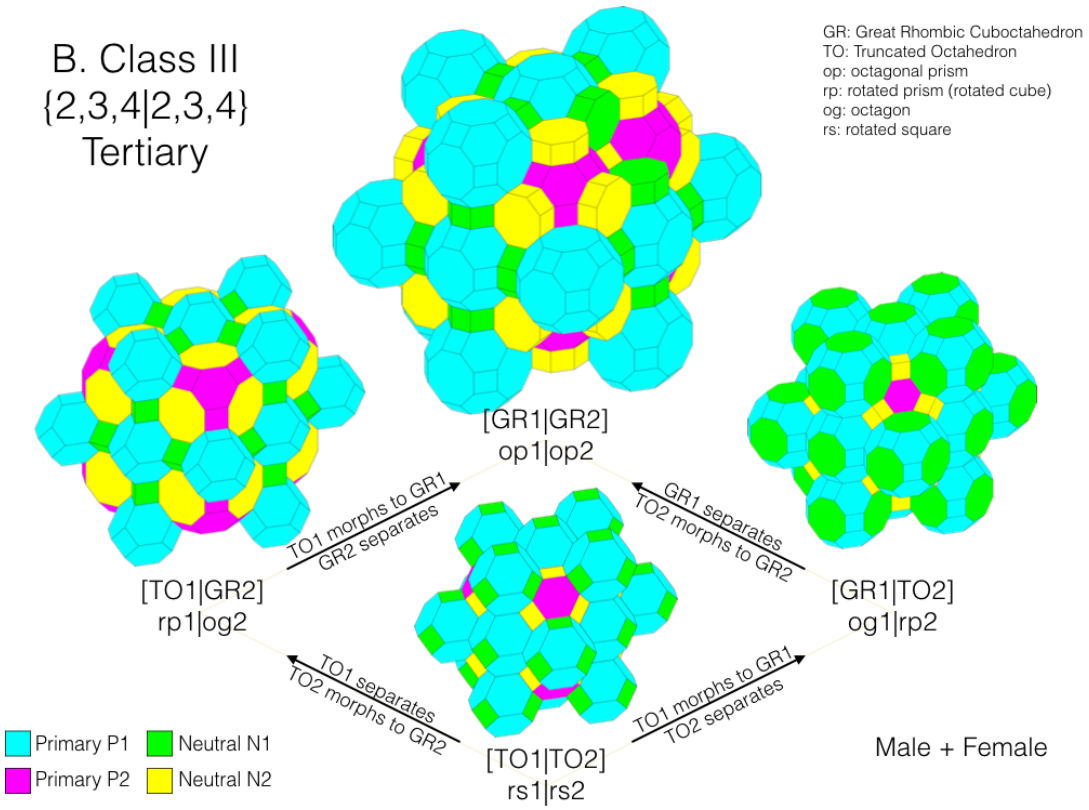
B. Class III
{2,3,4|2,3,4}
Tertiary
GR: Great Rhombic Cuboctahedron
TO: Truncated Octahedron
op: octagonal prism
rp: rotated prism (rotated cube)
og: octagon
rs: rotated square
[GR1|GR2]
op1|op2
[TO1|GR2]
rp1|og2
[GR1|TO2]
og1|rp2
[TO1|TO2]
rs1|rs2
TO1 morphs to GR1
GR2 separates
GR1 separates
TO2 morphs to GR2
TO1 separates
TO2 morphs to GR2
TO1 morphs to GR1
TO2 separates
Primary P1
Primary P2
Neutral N1
Neutral N2
Male + Female

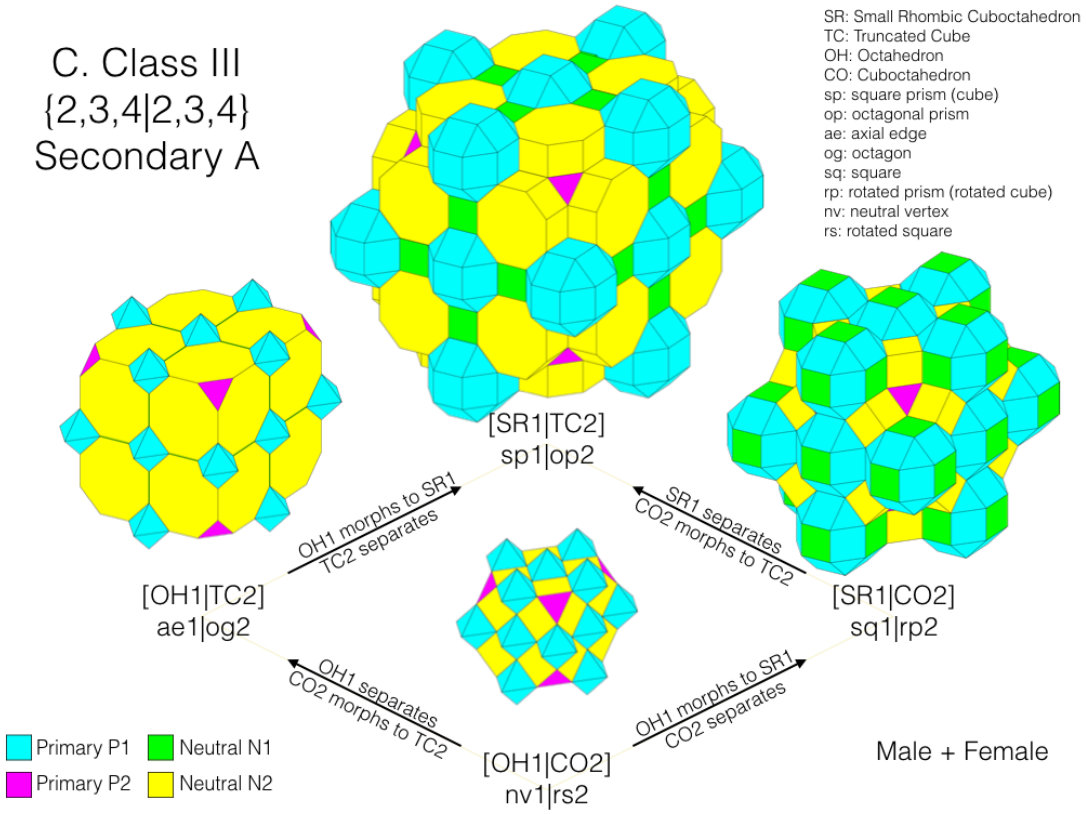
C. Class III
{2,3,4|2,3,4}
Secondary A
SR: Small Rhombic Cuboctahedron
TC: Truncated Cube
OH: Octahedron
CO: Cuboctahedron
sp: square prism (cube)
op: octagonal prism
ae: axial edge
og: octagon
sq: square
rp: rotated prism (rotated cube)
nv: neutral vertex
rs: rotated square
[SR1|TC2]
sp1|op2
[OH1|TC2]
ae1|og2
[SR1|CO2]
sq1|rp2
[OH1|CO2]
nv1|rs2
OH1 morphs to SR1
TC2 separates
SR1 separates
CO2 morphs to TC2
OH1 separates
CO2 morphs to TC2
OH1 morphs to SR1
CO2 separates
Primary P1
Primary P2
Neutral N1
Neutral N2
Male + Female

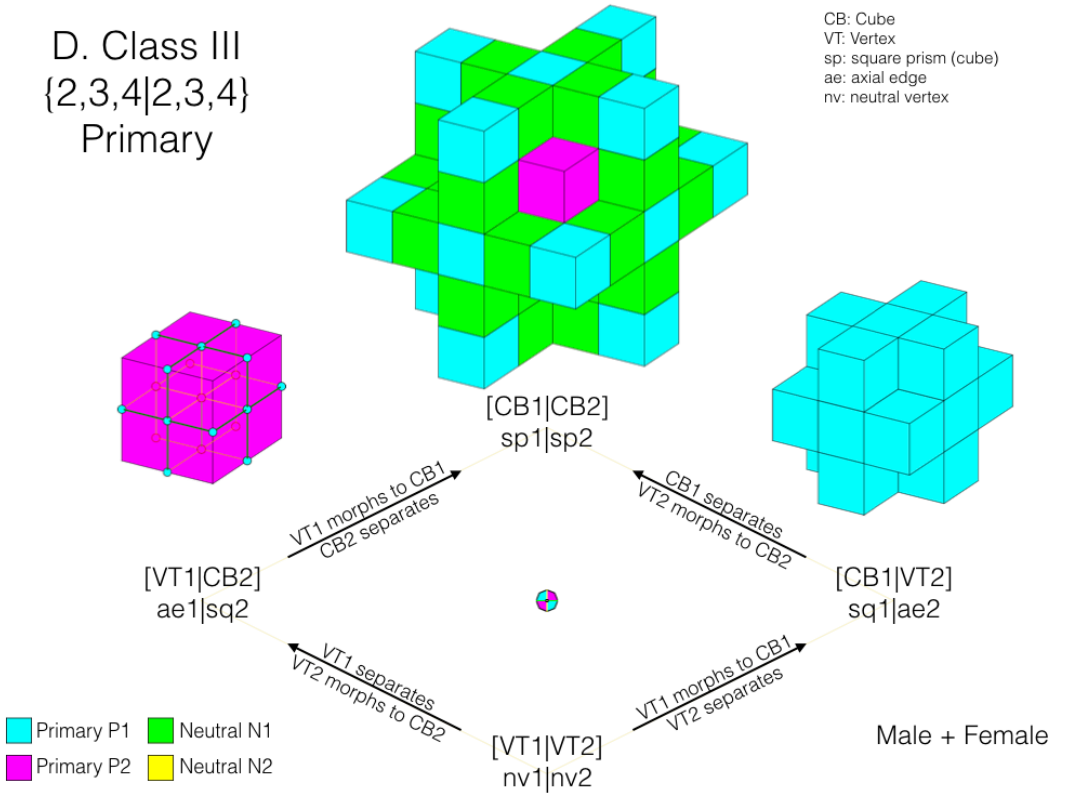
D. Class III
{2,3,4|2,3,4}
Primary
CB: Cube
VT: Vertex
sp: square prism (cube)
ae: axial edge
nv: neutral vertex
[CB1|CB2]
sp1|sp2
[VT1|CB2]
ae1|sq2
[CB1|VT2]
sq1|ae2
[VT1|VT2]
nv1|nv2
VT1 morphs to CB1
CB2 separates
CB1 separates
VT2 morphs to CB2
VT1 separates
VT2 morphs to CB2
VT1 morphs to CB1
VT2 separates
Primary P1
Primary P2
Neutral N1
Neutral N2
Male + Female

Figure 1: A: Class III {2,3,4|2,3,4} shows four sequence clusters of Primary (bottom), Secondary A (left) and its enantiomorph Secondary B (right), and Tertiary (top). Each sequence cluster separates from lower contracted state via two pathways to two middle intermediary states, which combine into upper expanded state. At each step, PP_1 and PP_2 take it in turn to either separate by unit edge length, or morph from one contracted PP to its expanded pair PP: VT to CB, OH to SR, CO to TC, or TO to GR. In those four fundamental morphs, the √3 faces of PP_1 or PP_2 separate by unit edge length, the √1 faces expand by the two fundamental expansions of VT to SQ, or RS to OG; and the √2 faces expand from VT to TE or DE to (√2-axial) SQ.

B: Class III Tertiary Sequence Cluster. In the first step, at left, from contracted form $[TO_1|TO_2]$, TO_1s separate and TO_2s morph to GR_2s, to yield intermediary $[TO_1|GR_2]$; while in the second step, TO_1s morph to GR_1s and GR_2s separate, to yield extended $[GR_1|GR_2]$. Right side is the enantiomorphic equivalent, as in the first step, TO_1s morph to GR_1s and TO_2s separate to yield intermediary $[GR_1|TO_2]$, while in the second step, GR_1s separate and TO_2s morph to GR_2s, to yield extended $[GR_1|GR_2]$.

C: Class III Secondary Sequence Cluster A. In the first step, at left, from contracted form $[OH_1|CO_2]$, OH_1s separate and CO_2s morph to TC_2s, to yield intermediary $[OH_1|TC_2]$; while in the second step, OH_1s morph to SR_1s and TC_2s separate, to yield extended $[SR_1|TC_2]$. Right side is the enantiomorphic equivalent, as in the first step, OH_1s morph to SR_1s and CO_2s separate to yield intermediary $[SR_1|CO_2]$, while in the second step, SR_1s separate and CO_2s morph to TC_2s, to yield extended $[SR_1|TC_2]$. Secondary Sequence Cluster B (not shown) is simply the enantiomorph of this sequence cluster.

D: Class III Primary Sequence Cluster. In the first step, at left, from contracted form $[VT_1|VT_2]$, VT_1s separate and VT_2s morph to CB_2s, to yield intermediary $[VT_1|CB_2]$; while in the second step, VT_1s morph to CB_1s and CB_2s separate, to yield extended $[CB_1|CB_2]$. Right side is the enantiomorphic equivalent, as in the first step, VT_1s morph to CB_1s and VT_2s separate to yield intermediary $[CB_1|VT_2]$, while in the second step, CB_1s separate and VT_2s morph to CB_2s, to yield extended $[CB_1|CB_2]$.

2.2. Class II

The {2,3,3|2,3,4} Class II honeycombs are constituted of one or other of the GEs in both +ve and –ve orientations, and 2 PPs that share the same √1 faces, and comprise four different one-step expansion/contraction sequences of honeycomb from contracted form to expanded form, and their respective NEs: $NE_{GE} = NE_T$ or NE_D, and NE_{PP}. Figure 2 shows that these sequences consist of two parallel one-step sequences, one for GE=$T^{+/-}$, and one for GE=$D^{+/-}$. Analogous to Class III, the step in either sequence is characterized by the set of GEs separating by unit distance, while the two PPs of the other set morph to the two other PPs. The four morphs are the same as for Class III. In a sequence, one reflective PP and one non-reflective PP of the contracted honeycomb morph to another reflective PP and another non-reflective PP, respectively, of the expanded honeycomb. GEs in the contracted honeycomb are contiguous, mediated by the NE of DE; while the two PPs are contiguous, mediated by the NE of NV or RS. In the expansion, the GEs separate by unit distance along the XYZ axes, the neutral DEs projecting along their primary XYZ axis to become DPs; while the two PPs morph to two other PPs, as their NEs expand from NV to NS or RS to OG. Figure 3 shows the PPs OH and VT morphing to SR and CB (Fig. 3 A), and TO and CO morphing to GR and TC (Fig. 3 B) (though the morph VT to CB might better be described as an expansion).

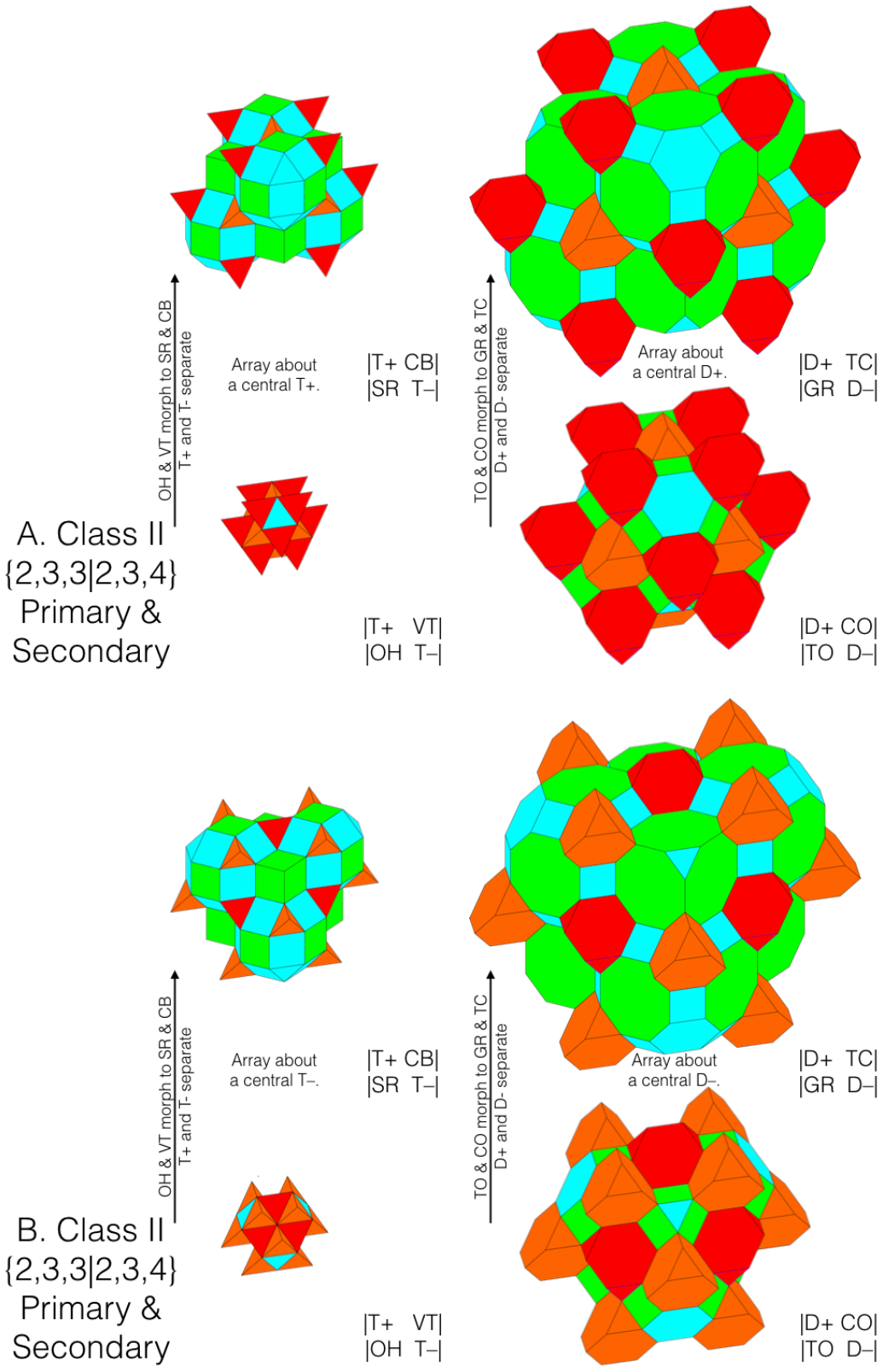

Figure 2: Class II {2,3,3|2,3,4} shows two parallel sequences of Primary (left), and Secondary A (right). In the Primary sequence at left, from the contracted $\begin{vmatrix} T^+ & VT \\ OH & T^- \end{vmatrix}$ (bottom), T^+ and T^- separate, while OH

and VT morph into SR and CB, respectively, to yield the expanded $\left|\begin{matrix} T^+ & CB \\ SR & T^- \end{matrix}\right|$ (top). This is paralleled in the Secondary sequence at right, where from the contracted $\left|\begin{matrix} D^+ & CO \\ TO & D^- \end{matrix}\right|$ (bottom), D^+ and D^- separate, while TO and CO morph into GR and TC, respectively, to yield the expanded $\left|\begin{matrix} D^+ & TC \\ GR & D^- \end{matrix}\right|$ (top). A. Cluster about a core T^+, and B. cluster about a core T^-.

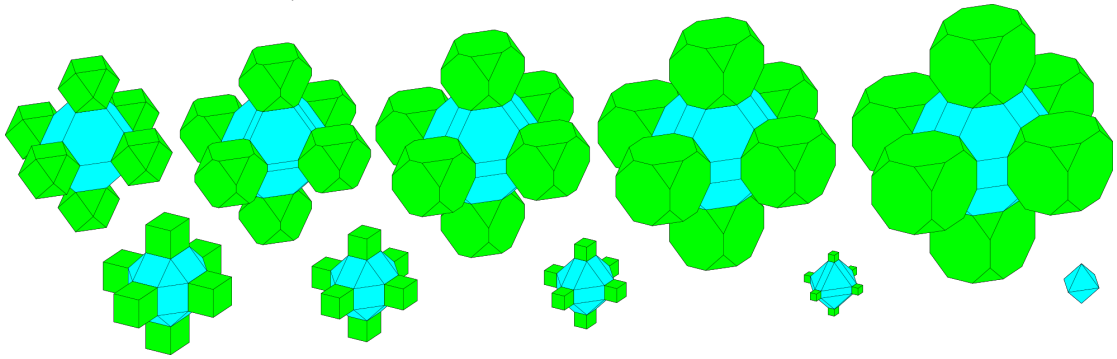

Figure 3: Class II Morphs: A. (above, left-to-right) $TO + CO$ morph to $GR + TC$. NEs mediating PPs expand RS to OG (not shown). B. (below, right-to-left) $OH + VT$ morph to $SR + CB$. NEs mediating PPs expand NV to SQ (not shown).

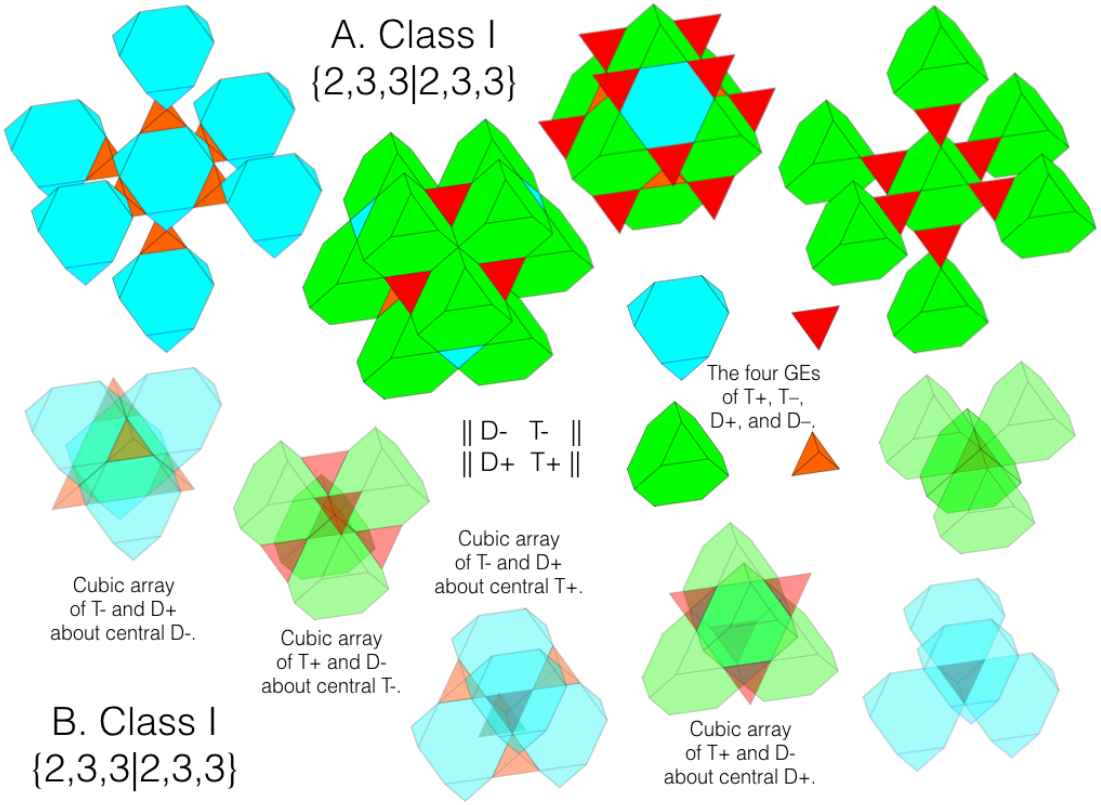

Figure 4: Class I {2,3,3|2,3,3}. In this singular honeycomb, all four GEs of T^+, T^-, D^+, and D^- alternate with one another, and PPs do not appear. This is the most profound of the all-space-filling periodic honeycombs. A. (upper) Various views, and the four GEs. B. (lower) Various views clustering about a core $T^{+/-}$ or $D^{+/-}$, with 50 % transparency. C. (next page) The honeycomb consists of two types of axial strands along XYZ axes, alternating either edge-jointed T^+ and D^- (red/green), or edge-jointed T^- and D^+ (orange/blue). Views are shown of strands intersecting at a central $T^{+/-}$ or $D^{+/-}$.

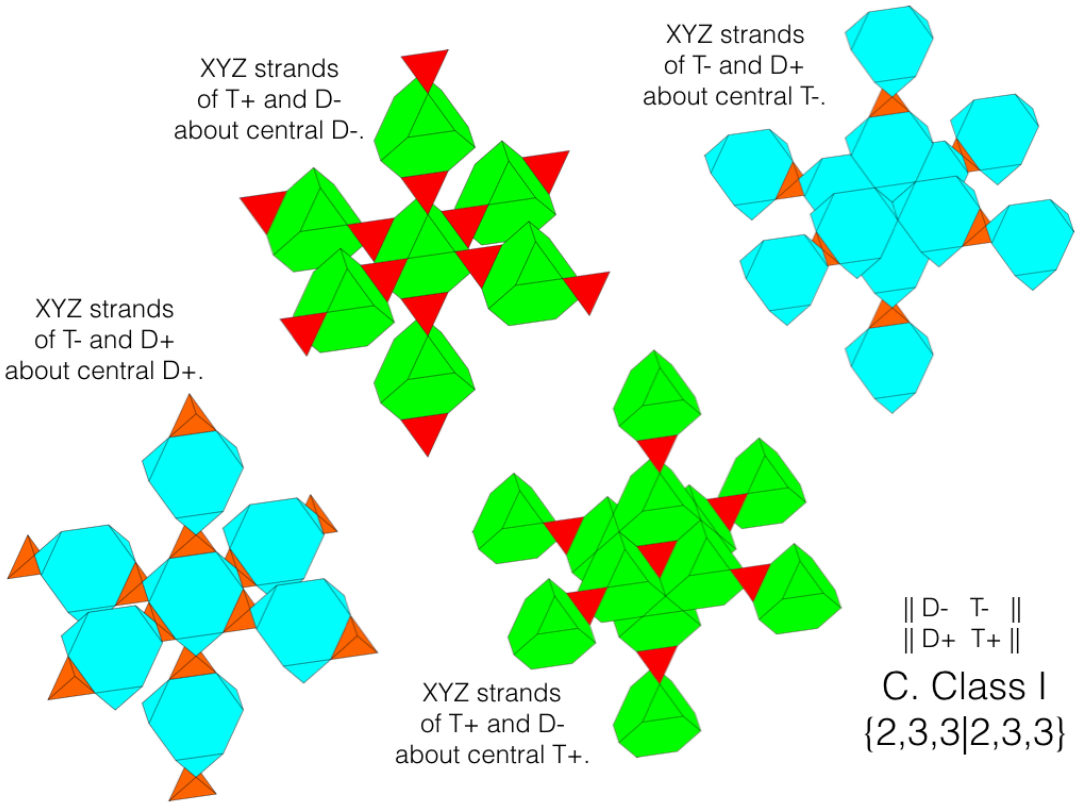

2.3. Class I

Figures 4 A and B (previous page) show that the {2,3,3|2,3,3} Class I honeycomb is constituted of both GEs in both +ve and –ve orientations, and their respective NEs = DP. This class thus shows no expansion/contraction sequences of honeycombs from contracted form to expanded form. Figure 4 C (above) shows that the GEs D^+ and T^- alternate along the axes of RCL_1, and are contiguous, though mediated by their NE of DE transverse to their primary XYZ axis, of alternating orientation. Meanwhile, D^- and T^+ alternate along RCL_2, and are also contiguous, though mediated by their NE of DE transverse to their primary XYZ axis, of alternating orientation.

2.4. Subsets of polytopes of all three classes

This analysis means that the constituent polytopes of any of these honeycombs may be differentiated into subsets of polytopes, as follows: Class III: one (self-reflective) or two PPs, and their respective NEs; Class II: one or other GE in both orientations GE^+ and GE^- and 2 PPs, and their respective NEs (which are at maximum, 2D); and Class I: characterized by 2 (both) GEs in both +ve and –ve orientations, i.e. $RT_1^{\alpha} = D_1^+$, $RT_1^{\beta} = T_1^-$, $RT_2^{\alpha} = T_2^+$, $RT_2^{\beta} = D_2^-$; and their respective $NE_{GE}^{+/-}$s. The NE can be divided into NE_1 and NE_2, which can be differentiated as: NE_1^X, NE_1^Y, NE_1^Z, and NE_2^X, NE_2^Y, NE_2^Z; and as +ve or –ve, according to their axial direction.

Class II is characterized by $RT_1^{\alpha} = T_1^+$ or D_1^+, $RT_1^{\beta} = T_1^-$ or D_1^-, $RT_2^{\alpha} = PP_2^+$, $RT_2^{\beta} = PP_2^-$, where for a specific honeycomb, "or" is exclusive; and PP^+ and PP^- are NOT the same polyhedron, but are rather √1 complementary – the two PPs that exhibit the same √1 face.

Class III can be rectified to a similar 4-fold alternation of tetrahedral lattices by considering the colorings of both PPs, where the "coloring" differentiates +/– pairs of either PP according to their α/β location, so that Class III is characterized by $RT_1^{\alpha} = PP_1^{+}$, $RT_1^{\beta} = PP_1^{-}$, $RT_2^{\alpha} = PP_2^{+}$, $RT_2^{\beta} = PP_2^{-}$. In the four self-reflective Class III honeycombs, $PP_1 = PP_2$ (i.e. all 4 polyhedra are the same polyhedron, but in different locations). The remaining six non-self-reflective honeycombs, $PP_1 \neq PP_2$ can be further differentiated into the two arrays of two different self-reflective PPs (where the two PPs are √3 identical, $[GR|TO]$ and $[CB|VT]$, sharing the same HG or $V3$ hexagon or vertex √3 face, respectively), and the four arrays of different non-self-reflective PPs (where the two polyhedra are instead √3 complementary, $[OH|CO]$, $[CO|SR]$, $[SR|TC]$, and $[TC|OH]$, sharing the complementary, hence mating, TR^{+} Δ or TR^{-} ∇ triangular 180° rotated √3 face).

So Class I may be considered as the four-fold alternation of 4 interpenetrating tetrahedral lattices of both GEs of both orientations; Class II as the alternation of alternation of two pairs of interpenetrating tetrahedral lattices, one pair being GEs and the other pair being √1 complementary PPs $VT:OH$, $CO:TO$; $CB:SR$; $TC:GR$; and Class III the alternation of alternation of two pairs of interpenetrating tetrahedral lattices, where either pair consists of the same PP; but the two PPs of RCL_1 and RCL_2 are √3 mating PPs, which in the contacted and expanded honeycombs of the primary and tertiary sequences are the same PP, but in the intermediary forms of those two sequences and in the entire secondary sequence differ.

3. Form and Counterform Arrays

Having deposed the polyhedra of the periodic honeycombs into classes and into the constituent sets and locations, and identified neutral polytopes that can be considered to separate the GEs and PPs, the arrays of combinations of these constituent sets can be addressed. Of course any combination of the constituent sets of polyhedra and neutral polytopes of a honeycomb, or more generally its class, can be considered, and for Classes II and III, in regard to its sequence – and abstracted across sequences. But the present enquiry is concerned with form and counterform. In both classes, form and counterform are characterized by contiguity, even though that contiguity might only be through mediating VT, TE, DE, AE, or DP; and together, form and counterform fill all space, so that they consist of interpenetrating arrays that share a common (two-sided) surface. Notwithstanding this approach, practical applications might well consider configurations where one or other are not contiguous; a contiguous form might serve as the reticulated provision of services and service spaces, while the counterform might be discrete (non-contiguous) usable, even habitable spaces – or at the organic level, artificial bone tissue scaffolding and discrete pores. Or the use of three or more interpenetrating arrays might be considered. But in this paper, only the all-space-filling combinations of just two arrays are addressed. These reveal common structure over the three Classes, and are identified according to axes of contiguity, and class.

3.1. √1 XYZ Axes of Contiguity

3.1.1. √1 Axes of Contiguity for Class III.

The inspiration for the exploration of form and counterform came from the cubic array formed by core cubes in face-to-face contact with intermediary cubes, so that each core cube

is in face-to-face contact with six intermediary cubes, while each intermediary cube is in face-to-face contact with two core cubes, one at each end. This might be regarded as an archetypal form; the leftover space, the "exterior", proves to be precisely the same array (though displaced). So the common surface of squares separates two arrays that here are identical. Space is divided into two interpenetrating compartments, the exterior of one being the interior of the other. One is form, the other counterform. The metaorder of honeycombs I advance subsumes this as a division of the $[CB_1 \mid CB_2]^{SP_2}_{SP_1}$ expanded array of the primary sequence in Class III, with CB_1 and its neutral SP_1 as form, and CB_2 and its neutral SP_2 as counterform.

In general, form and counterform (CNTR) for the Class III √1 axes of contiguity can be:
FORM | CNTR: $<PP_1 : NE_1 : PP_1> \mid <PP_2 : NE_2 : PP_2>$. Hence, Table 1:

Table 1. Class III √1 Honeycombs and Contiguous Form and Counterform Arrays.

Honeycomb	FORM array	CNTR array	Sequence	EXP
$[GR_1 \mid GR_2]^{OP_2}_{OP_1}$	$<GR_1 : OP_1 : GR_1>$	$<GR_2 : OP_2 : GR_2>$	Tertiary	2
$[TO_1 \mid GR_2]^{OG_2}_{RP_1}$	$<TO_1 : RP_1 : TO_1>$	$<GR_2 : OG_2 : GR_2>$		1
$[TO_1 \mid TO_2]^{RS_2}_{RS_1}$	$<TO_1 : RS_1 : TO_1>$	$<TO_2 : RS_2 : TO_2>$		0
$[SR_1 \mid TC_2]^{OP_2}_{OP_1}$	$<SR_1 : OP_1 : SR_1>$	$<TC_2 : OP_2 : TC_2>$	Secondary	2
$[OH_1 \mid TC_2]^{OG_2}_{AE_1}$	$<OH_1 : AE_1 : OH_1>$	$<TC_2 : OG_2 : TC_2>$		1
$[SR_1 \mid CO_2]^{RP_2}_{SQ_1}$	$<SR_1 : SQ_1 : SR_1>$	$<CO_2 : RP_2 : CO_2>$		1
$[OH_1 \mid CO_2]^{RS_2}_{VT_1}$	$<OH_1 : VT_1 : OH_1>$	$<CO_2 : RS_2 : CO_2>$		0
$[CB_1 \mid CB_2]^{SP_2}_{SP_1}$	$<CB_1 : SP_1 : CB_1>$	$<CB_2 : SP_2 : CB_2>$	Primary	2
$[VT_1 \mid CB_2]^{SQ_2}_{AE_1}$	$<VT_1 : AE_1 : VT_1>$	$<CB_2 : SQ_2 : CB_2>$		1
$[VT_1 \mid VT_2]^{NV_2}_{NV_1}$	$<VT_1 : NV_1 : VT_1>$	$<VT_2 : NV_2 : VT_2>$		0

Notes: Exp: Degree of Expansion: 2: Expanded; 1: Intermediary; 0: Contracted.

Therefore, within Class III, for either RCL, each PP appears in two different cubic arrays, in either contracted adjoining) or expanded (adjacent) form, and each of these arrays (together with its NEs) can conveniently be considered as form or counterform, as in Figs. 5–8, where male and female can refer to form and counterform (or *vice versa*). Note the alternative separation and morphing of pairs of PP_1 and PP_2 at each step of the expansion sequences, so that in the first step PP_1 separates while PP_2 morphs, then in the second step the opposite of PP_1 morphing while PP_2 separates; or the converse of in the first step PP_1 morphs while PP_2 separates, then in the second step the opposite of PP_1 separating while PP_2 morphs.

This *do-si-doing* motif appears fundamental to the honeycomb sequences, and can also be recognized in the relationship of the faces of the individual polyhedra in a symmetry class, e.g. of the Class II {2,3,4} polyhedra that are also the honeycomb PPs, and which I intend to address in a later paper that will revise my earlier New Order in Space [10].

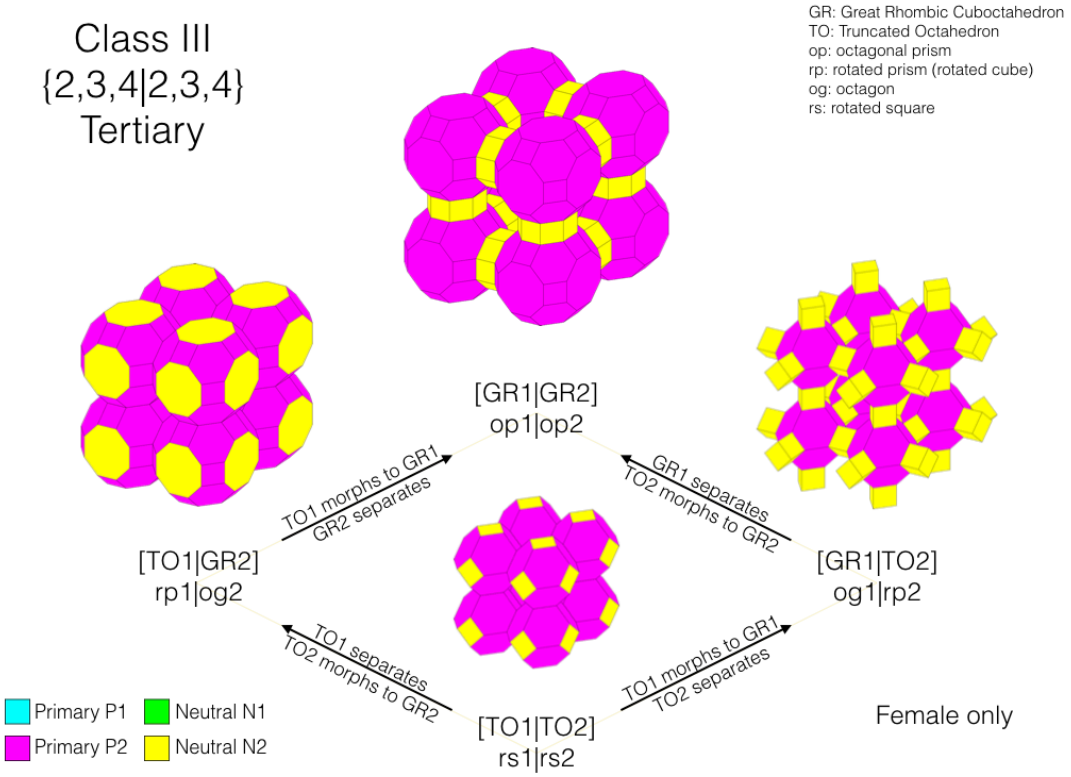

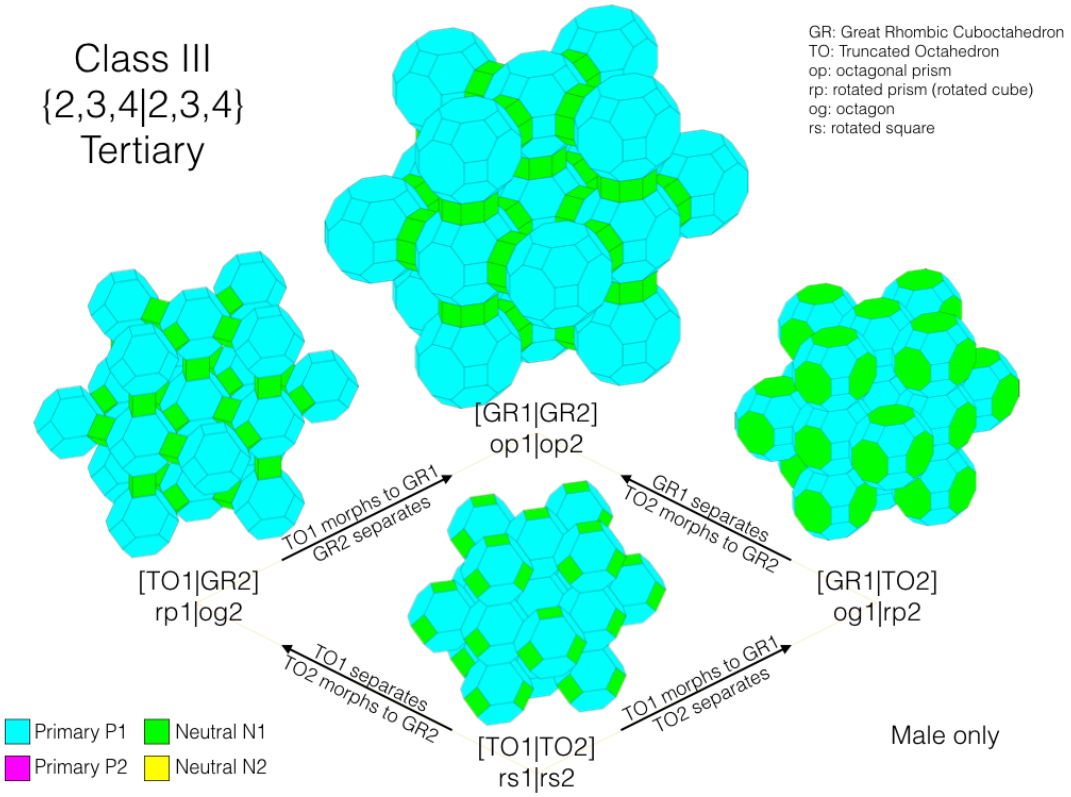

Figure 5: Class III Tertiary sequence cluster of Female & Male form/counterform for √1 axes.

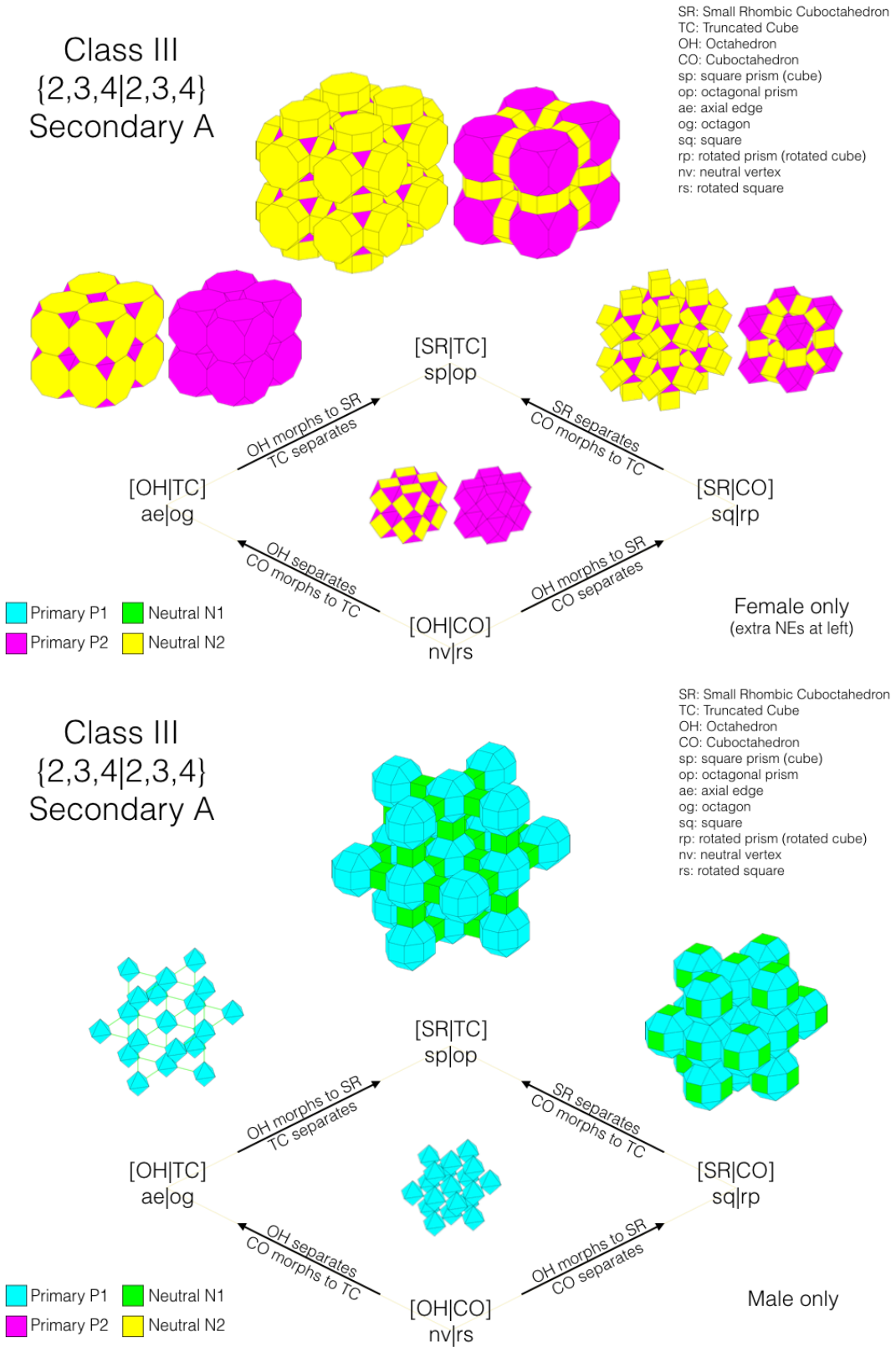

Figure 6: Class III Secondary A sequence cluster of Female & Male form/counterform for √1 axes. Secondary B sequence cluster (not shown) is the enantiomorph of Secondary A cluster.

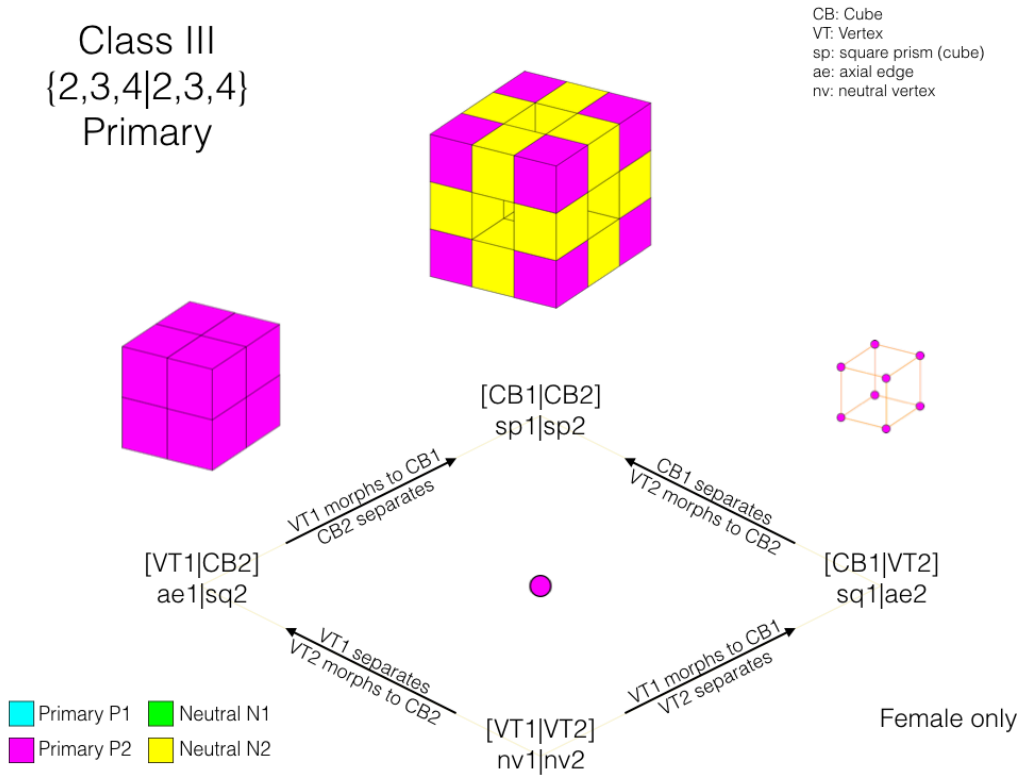

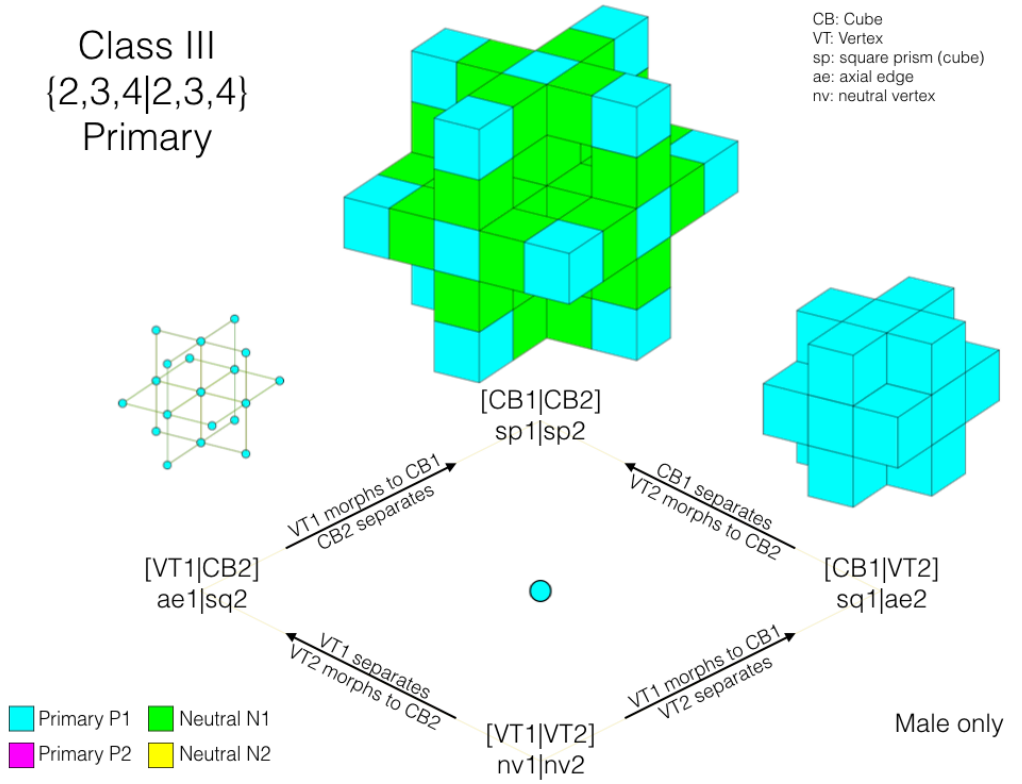

Figure 7: Class III Primary sequence cluster of Female & Male form/counterform for √1 axes. $[CB_1|CB_2]$ alternates $CB + sp$ with $CB + sp$; $[CB_1|VT_2]$ alternates $CB + sq$ with $VT + nv$.

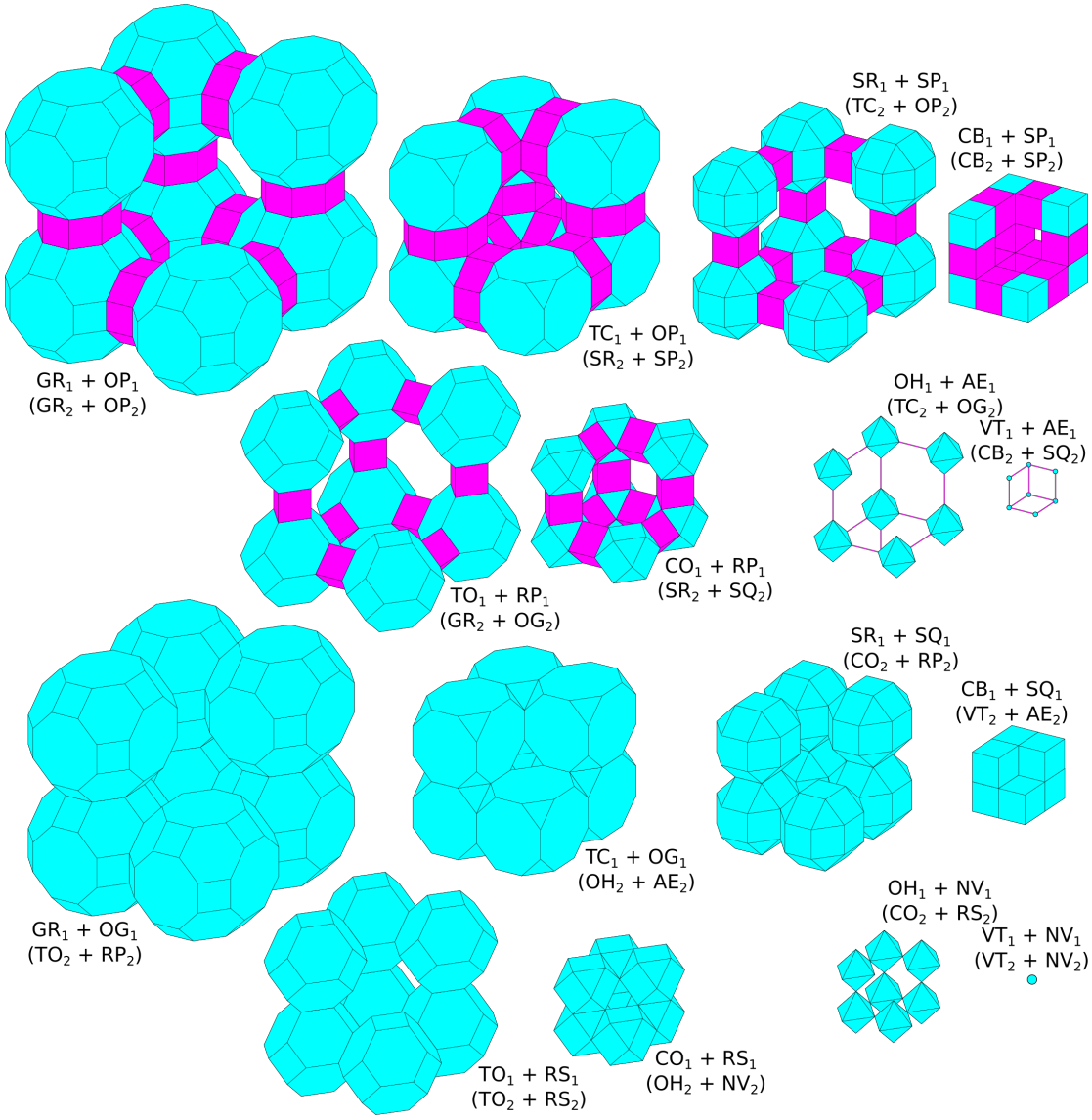

Figure 8. A. (Top two rows of polyhedral arrays). Pairs of Class III cubic arrays of *PPs* in expanded form for √1 axes. Top line of label is given form; bottom line is virtual counterform (also shown either here or in Fig. 8 B as form, as some honeycombs combine contracted and expanded cubic arrays of *PP*s; both forms and counterforms also shown in Figs. 5–7). Each *PP* array occurs once as given form, and once as virtual counterform. Seven of the eight *PPs* of one reference cube are shown (in blue); given neutral elements from bottom to top are 2 each of AE, RP, SP, or OP (in magenta). Each contracted (Fig. 8 B) or expanded (Fig. 8 A) array could be considered as form, or counterform. Note rigorous correspondence between each Fig. 8 A array (above) as expanded equivalent of corresponding contracted Fig. 8 B array (below). For color, refer SI at http://www.rmeurant.com/its/si-4.html .

B: (Bottom two rows of polyhedral arrays). Pairs of Class III cubic arrays of *PP*s in contracted form for √1 axes. Top line of label is given form as $PP_1 + NE_1$; bottom line is virtual counterform as $PP_2 + NE_2$ (also shown here or in Fig. 8 A as form; both forms and counterforms also shown in Figs. 5–7). Each *PP* array occurs once as given form, and once as virtual counterform. Seven of the 8 *PP*s of one reference cube are shown; given neutral elements are 2 each of (here uncolored) NV, RS, SQ, or OG.

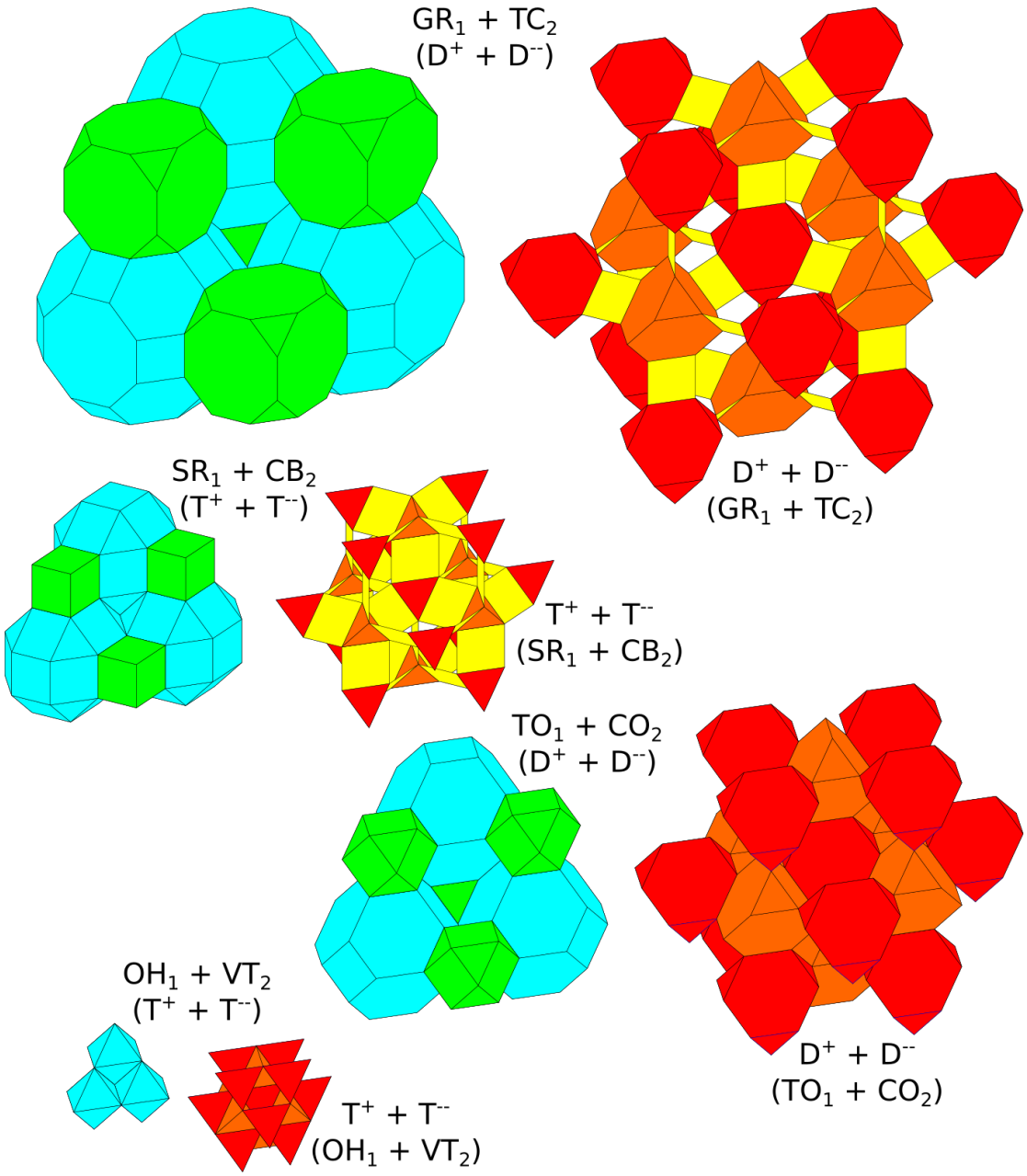

Figure 9. (a) Class II cubic arrays of PPs and GEs in contracted (lower) and expanded (upper) form. Top and bottom lines are given form and virtual counterform for √1 axes, respectively. For clarity, only 7 of the 8 PPs of one reference cube are shown: only 3 of 4 PP_1 in (–ve) tetrahedral array (blue) and 4 PP_2 in (+ve) tetrahedral array (green). All GEs are shown in cuboctahedral (+ve, red) and octahedral (–ve, orange) array about a core GE^+ (red), with neutral 2-D DPs in yellow. All configurations repeat indefinitely, and each could be considered as form, or counterform.

3.1.2. √1 Axes of Contiguity for Class II.

Figure 9 shows that form and counterform for the √1 Axes of Contiguity for Class II can be:

FORM | CNTR: $<GE_1^+ : NE_{GE} : GE_1^->$ | $<PP_2^+ : NE_{PP} : PP_2^->$

where, PP_2^+ and PP_2^- are complementary PPs pairs sharing the same √1 face. Hence, Table 2:

Table 2. Class II √1 Honeycombs and Contiguous Form and Counterform Arrays.

Honeycomb	FORM array	CNTR array	FORM array	CNTR array	Honeycomb
$\begin{vmatrix} T^+ & CB \\ SR & T^- \end{vmatrix}$	$<T_1^+ : DE : T_1^->$	$<CB_2^+ : SQ_2 : SR_2^->$	$<D_1^+ : DE : D_1^->$	$<TC_2^+ : RS_2 : GR_2^->$	$\begin{vmatrix} D^+ & TC \\ GR & D^- \end{vmatrix}$
$\begin{vmatrix} T^+ & VT \\ OH & T^- \end{vmatrix}$	$<T_1^+ : DE : T_1^->$	$<VT_2^+ : NV_2 : OH_2^->$	$<D_1^+ : DE : D_1^->$	$<CO_2^+ : RS_2 : TO_2^->$	$\begin{vmatrix} D^+ & CO \\ TO & D^- \end{vmatrix}$

3.1.3. √1 Axes of Contiguity for Class I.

In general, the form and counterform for the √1 Axes of Contiguity for Class I, as shown in Fig. 11 (right), can be:

FORM | CNTR: $<GE_1^+ : NE_1 : GE_1^-> | <GE_2^+ : NE_2 : GE_2^->$

i.e., FORM | CNTR: $<D_1^+ : DE_1 : T_1^-> | <T_2^+ : DE_2 : D_2^->$

where, D_1^+ and T_1^- alternate to form chains of GEs along the √1 XYZ axes of RCL_1, while, T_2^+ and D_2^- alternate to form chains of GEs along the √1 XYZ axes of RCL_2. These chains are shown earlier in Fig. 4 C.

3.2. √2 XYZ Axes of Contiguity

I do not here consider the √2 XYZ Axes of Contiguity form and counterform arrays.

3.3. √3 XYZ Axes of Contiguity

Note that these are dealt with in different order.

3.3.1. √3 Axes of Contiguity for Class I.

In the Class I honeycomb, D^+ on its triangular faces only mates with T^+ (the reduced size of the parent T it is truncated from), while D^- on its triangular faces only mates with T^-, to form interpenetrating arrays of $<D_1^+ - T_2^+>$ and $<D_2^- - T_1^->$. Therefore, as shown in Fig. 11 (left):

FORM | CNTR: $<D_1^+ : TR_{12} : T_2^+> | <D_2^- : TR_{21} : T_1^->$

This is an interesting pair of arrays, as either might be considered to consist of the array of 3-frequency T^+/T^- formed by D^+/D^- and T^+/T^-, which 3f T^+/T^- overlap at common T^+/T^-.

Alternatively, D^+ on its hexagonal faces only mates with D^-, while T_2^+ on its vertex faces (its vertices) only mates with T_1^- to form interpenetrating arrays of $D^{+/-}$, and of $T^{+/-}$. Therefore, as shown in Fig. 11 (center):

FORM | CNTR: $<D_1^+ : HG_{12} : D_2^-> | <T_2^+ : HG_{21} : T_1^->$

3.3.2. √3 Axes of Contiguity for Class II.

In Class II, PP alternates along its √3 axes in the order $(PP^+ - GE^+ - PP^- - GE^-) = (VT^{\alpha}: NV^+: T^+: TR^+: OH^-: TR^-: T^-: NV^-) + (CO^{\alpha}: TR^+: D^+: HG^+: TO^-: HG^-: D^-: TR^-)$, $(CB^{\alpha}: NV^+: T^+: TR^+: SR^-: TR^-: T^-: NV^-) + (TC^+: TR^+: D^+: HG^+: GR^-: HG^-: D^-: TR^-)$, for the contracted, and the expanded forms, respectively (where the +/– designations of the NEs are not rigorous, but indicative only). Form and counterform can be obtained by associating GE^+ with PP^+, and GE^- with PP^-, or alternatively, GE^+ with PP^-, and GE^- with PP^+:

FORM | CNTR: $<GE_1^+ - PP_2^+> | <GE_1^- - PP_2^->$, or, $<GE_1^+ - PP_2^-> | <GE_1^- - PP_2^+>$

PP_2^+ and PP_2^- are not the same polyhedra, but complementary PP pairs with the same √1 face. These are shown in Fig. 10:

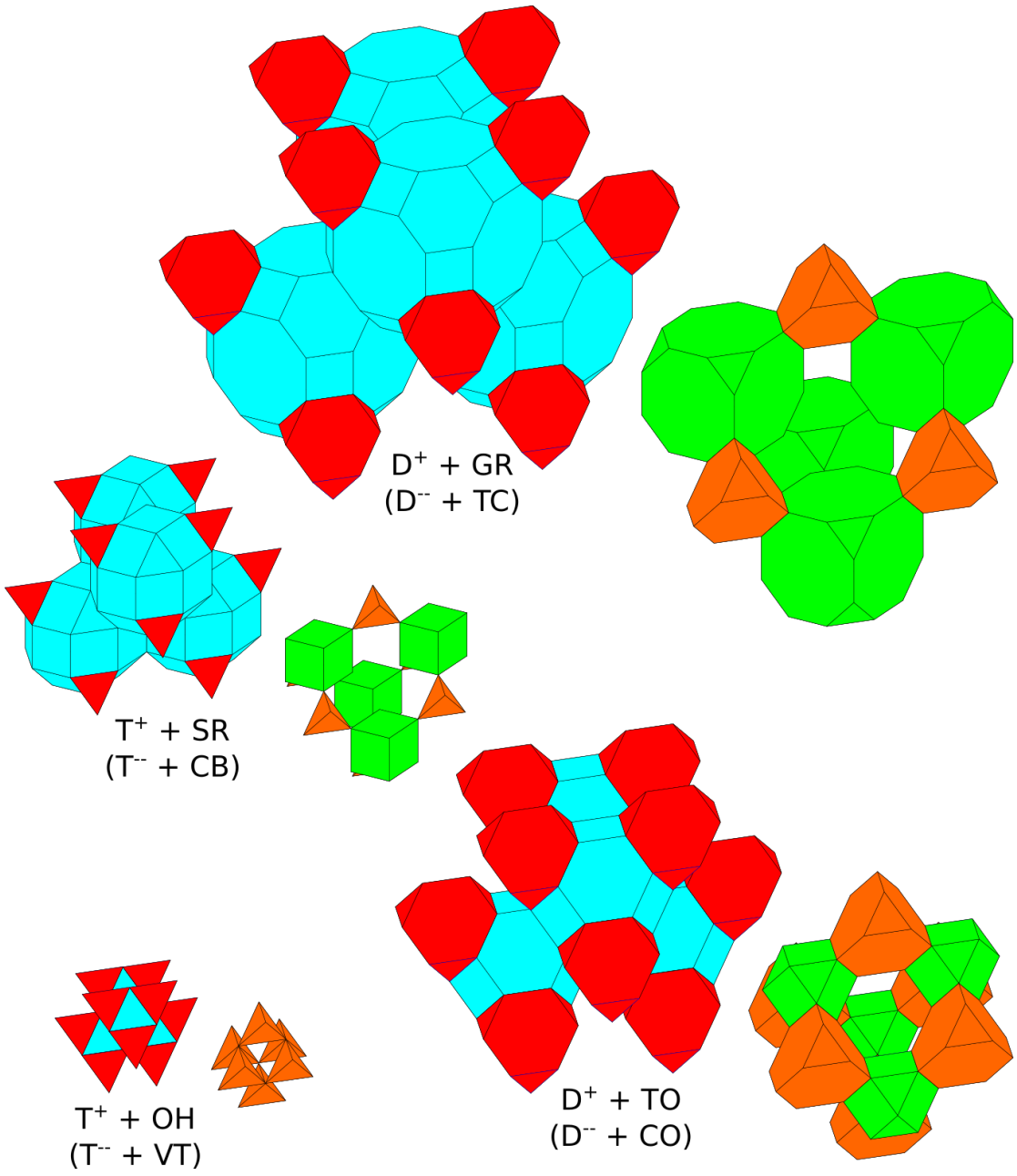

Figure 10: Class II Form and Counterform for √3 axes showing GE^+ (red) + PP_1 (blue) as Form and GE^- (orange) + PP_2 (green). GE^+ in cuboctahedral array, PP_1 in (–ve) tetrahedral array, GE^- in octahedral array, and PP_2 in (+ve) tetrahedral array, all around a core GE^+ (not shown in $GE^- + PP_2$). Top to bottom: Form and counterform are 1. Expanded $D^+ + GR_1$ and $D^- + TC_2$; 2. Expanded $T^+ + SR_1$ and $T^- + CB_2$; 3. Contracted $D^+ + TO_1$ and $D^- + CO_2$; and 4. Contracted $T^+ + OH_1$ and $D^- + VT_2$. $T^+ + OH_1$ and $D^- + VT_2$ expand to $T^+ + SR_1$ and $T^- + CB_2$; $D^+ + TO_1$ and $D^- + CO_2$ expand to $D^+ + GR_1$ and $D^- + TC_2$. $T^+ + OH_1$ and $D^- + VT_2$. All configurations repeat indefinitely. For color, refer SI at http://www.rmeurant.com/its/si-4.html .

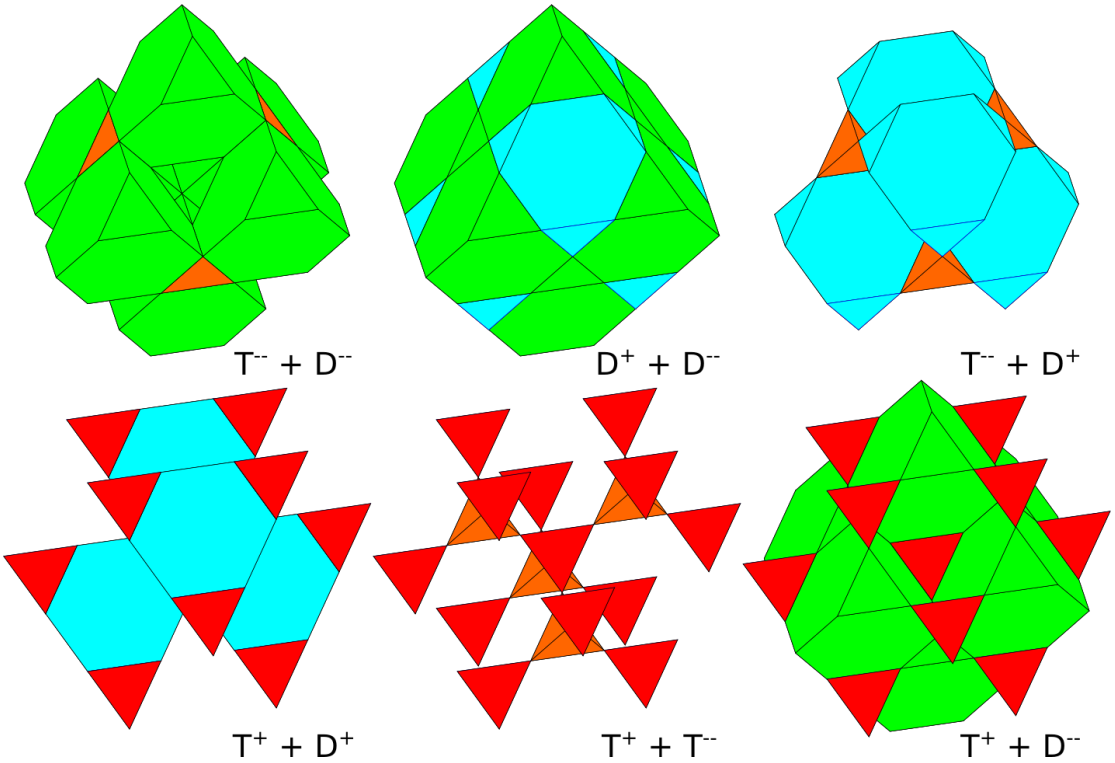

Figure 11: Class I Form (below) and Counterform (above) for $T^+ + D^+$ and $T^- + D^-$ (left); $T^+ + T^-$ and $D^+ + D^-$ (center); and $T^+ + D^-$ and $T^- + D^+$ (right). Various combinations of cuboctahedral array of T^+ (red, –ve) tetrahedral array of D^+ (blue, +ve) tetrahedral array of T^- (orange), and octahedral array of D^- (green), all around a core T^+ (red, not shown above), obscured at below left). All configurations repeat indefinitely. For color, refer SI at http://www.rmeurant.com/its/si-4.html .

3.3.3. √3 Axes of Contiguity for Class III.

Class III honeycombs are realized in similar manner as employed in Class II, in this case by actualizing the coloring of PPs, so PP_1=$PP_1^+ + PP_1^-$ and PP_2=$PP_2^+ + PP_2^-$. Ignoring √1 NEs:

FORM | CNTR: $<PP_1^+ - PP_2^+>$ | $<PP_1^- - PP_2^->$ or $<PP_1^+ - PP_2^->$ | $<PP_1^- - PP_2^+>$

depending on which tetrahedral array of PP_1 is mated with which tetrahedral array of PP_2. This works without practical concern for the honeycombs that do not have 3D NEs by neglecting the √1 NEs, but needs to be taken account of in the honeycombs that do. This presents a formal problem, as it is not possible while maintaining true 3D symmetry, short of the formally unsatisfactory solution of dividing each NE into two.

4. Validation of the Metaorder

This research described in this paper applies the metaorder of the all-space-filling periodic polyhedral honeycombs derived by the author to explore the notion of form and counterform in these honeycombs. In so doing, it has validated this metaorder, while refining it and developing it where possible. The honeycomb metaorder reveals rigor and consistency in terms of the differentiation of the honeycombs into symmetry classes, and into the component sets of 2 pairs of GE polyhedra, 8 PP polytopes, and 10 (0, 1, 2, and 3)D √1 NE polytopes. The continuity of pattern through sequences within classes, from class to class, and the form–counterform dialectic they exhibit further confirms that the descriptive metaorder is a true,

fair, and accurate description of their order. At no stage of the investigations does a contradiction or formal inadequacy arise. That order necessitates the recognition of the VT as the null PP, the inclusion of the null $[VT_1|VT_2]$ honeycomb, as well as the "degenerate" $[VT_1|CB_2]$ honeycomb and its enantiomorph, the inclusion of (0, 1, and 2)D NEs as well as the 3D NEs, and the inclusion of the OP in the NEs. The inclusion of (0, 1, and 2)D NEs is both for convenience, and to allow complete description. When these various recognitions are made, the patterns become clearly consistent across all of the honeycombs.

The objection might be raised – what of the 3D chessboard consisting of alternating cubes and cubic spaces, where each cube is face-to-face with cubic void, and cubes are in vertex-to-vertex contact, with cubic voids similarly arrayed? But contemplation of this arrangement fully subsumes it as an instance of $[CB|VT]$, where the cubic array of cubes of RCL_1 is differentiated into two RTL_1s of cubes of different color, one being the "black/solid" cube of RTL_1^{α}, the other being the "white/empty" cubic void of RTL_1^{β}. These alternate throughout space, as conceptually do the two-colored VT_2^{α}s and VT_2^{β}s of $RCL_2 = RT_2^{\alpha}$, and RTL_2^{β}.

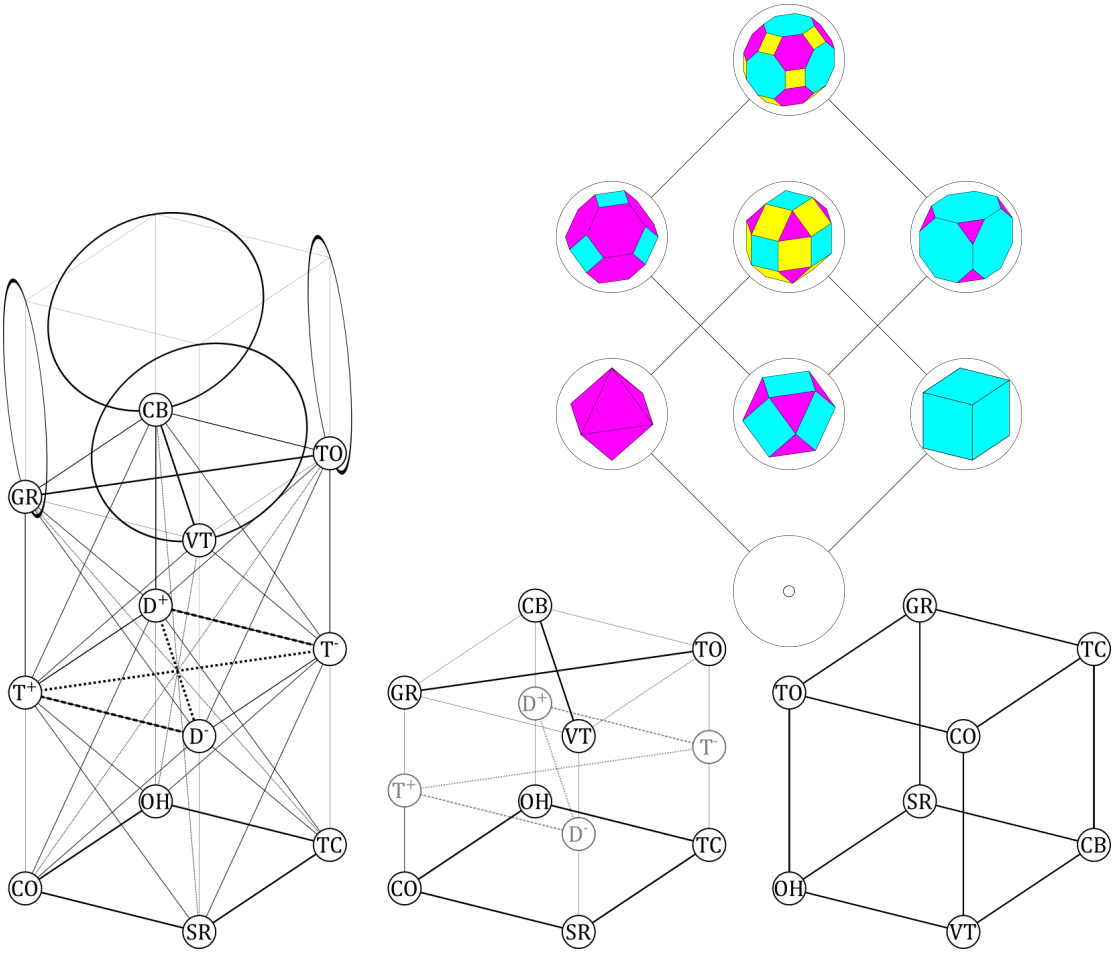

Figure 12: Left: The existent metaorder that codifies all 15 honeycombs (see Refs. [4: Fig. 5] and [6: Fig. 1]). Below middle: The abstracted cube of PPs of the existent metaorder. Top right (color) and below right: The proposed metaorder of the {2,3,4} regular and semi-regular polyhedra including the VT polytope, being the PPs of the honeycombs (see also Ref. [6: Fig. 7]). Reconciling these two cubic schema having regard to the individual polyhedra and the honeycombs is anticipated as future work.

5. Development of the Metaorder

Although the order of the constellation of honeycombs is now well understood and described, and their properties quite well characterized, the bicubic model of the GEs, PPs and honeycombs as previously advanced needs to be reformed, or at least further refined, and with consideration of the singular cubic model of the PPs (which manifests a different disposition of the PPs, see Fig. 12). This suggests the need to revise the author's earlier metaorder of the {2,3,3}, {2,3,4}, and {2,3,5} regular and semi-regular polyhedra (together with its extension into the {2,3,6} and {2,2,4} tessellations of the plane) [10–12], in order to accommodate the null polytope and $PP\ VT$, and to incorporate the corresponding VT in each class of that earlier metaorder, together with integrating the various implications. Despite this, the central intimation remains – that the metaorder of these beautiful honeycombs and their sophisticated regularity ought to be reflected in a key configuration, a schematic that adequately represents their formal structure – for which the bicubic model is but a pale comparison. It is anticipated that further work will incorporate the transformations between the eight PPs, and also the four GEs, and the deep formal analogy with the sequences and sequence clusters of the honeycombs, the patterns of separation and morphing, and concomitant projection and expansion of neutral elements, whether of polyhedra, or polygonal faces, in both 3D and 2D.

6. Conclusion

This paper describes the relationships that characterize the fundamental structure of these honeycombs, individually, in sequence, and as various instances of the same metaorder, in application to the phenomenon of form and counterform. The rigor and consistency found throughout this application serve to validate the metaorder. In a fundamental sense, this metaorder of the honeycombs embodies the inherent structure of empirical 3-D space, as do the regular and semi-regular polyhedra and their interrelationships. These descriptive explorations in experimental geometry serve to characterize the honeycombs and their metaorder, and allow these essential configurations to become conceivable, imageable, and practical. While the essential motivation of this research remains the exploration and mastery of the timeless formal nature of the honeycomb arrays, practical application also offers potential. For example, form and counterform of the honeycombs enable the facile structuring of interpenetrating but distinct spaces that could be engineered to provide controllable porous membrane surfaces that allow two domains to interact with one another through controllable high surface area interfaces. Through the metaorder, the geometry of the honeycombs and their sequences and sequence clusters becomes accessible to a wide range of diverse applications, such as tensile arrays in the sea and in Space stressed by pneumatic envelope; deployable folding structures, such as antennae and sensor networks; chemical compounds of hybrid composites; new nanoscale-engineered materials; metamaterials; filters; and artificial bone tissue scaffolding. Finally, in a world that appears beset by political stride, environmental pollution, global warming, and even the denial or would be relativization of truth, contemplation of the metaorder reveals the innate integrity of the space within which we exist, and mediates a sense of perfection through timeless harmony that can serve to ameliorate the frustrations and limitations of our fragile existence.

***

7. References

1. R.C. Meurant, Form and Counterform in the All Space-filling Periodic Polyhedral Honeycombs, in L. Li and C.-C. Hung (eds.), *Proceedings of The Ninth International Conference on Information*, Tokyo, December 7–9, 2018, 51–56.
   PDF 65 at http://www.rmeurant.com/its/papers/polygon-1.html

2. R.C. Meurant, Towards a New Order of the Polyhedral Honeycombs: Part I: The New Order Introduced, FGCN: The 2012 International Conference on Future Generation Communication and Networking: DCA: The 2012 International Conference on Digital Contents and Applications. T.-h. Kim et al. (Eds.): FGCN/DCA 2012, CCIS 350, 217–225, 2012. Springer-Verlag Berlin Heidelberg 2012. PDF 57 at http://www.rmeurant.com/its/papers/polygon-1.html

3. R.C. Meurant, Towards a New Order of the Polyhedral Honeycombs: Part II: Who Dances with Whom?, in L. Li and T.-W. Kuo (eds.), *Proceedings of The Seventh International Conference on Information,* Taipei, Nov. 25–28, 2015, 369–373.
   PDF 61 at http://www.rmeurant.com/its/papers/polygon-1.html

4. R.C. Meurant, Towards a MetaOrder of the All-Space-Filling Polyhedral Honeycombs through the Mating of Primary Polyhedra, *Information* 19: 6(B), June 2016, 2111–2124.
   PDF 62 at http://www.rmeurant.com/its/papers/polygon-1.html

5. R.C. Meurant, Sequences of the All Space-filling Periodic Polyhedral Honeycombs, in L. Li and Chih-Cheng Hung (eds.), *Proceedings of the Eighth International Conference on Information*, Tokyo, May 17–19, 2017, 151–154.
   PDF 63 at http://www.rmeurant.com/its/papers/polygon-1.html

6. R.C. Meurant, Expansion Sequences and their Clusters of the All Space-filling Periodic Polyhedral Honeycombs, Information Journal, International Information Institute, Vol.20, No.10(A), Oct. 2017, 7345–7362; PDF 64 at http://www.rmeurant.com/its/papers/polygon-1.html

7. K. Critchlow, Order in Space. Thames and Hudson, London (1969).

8. B. Grünbaum, Uniform Tilings of 3-space. Geombinatorics 4, 49–56 (1994).

9. G. Inchbald, The Archimedean Honeycomb duals. The Mathematical Gazette 81, 213–219 (1997).

10. R.C. Meurant, A New Order in Space - Aspects of a Three-fold Ordering of the Fundamental Symmetries of Empirical Space, as evidenced in the Platonic and Archimedean Polyhedra - Together with a Two-fold Extension of the Order to include the Regular and Semi-regular Tilings of the Planar Surface, International Journal of Space Structures, vol. 6, no. 1, (1991), University of Surrey, Essex, 11–32; PDF 06 at http://www.rmeurant.com/its/papers/polygon-1.html

11. R.C. Meurant, The Tetraktys of Polyhedra – Their Harmonic Structure According to Traditional Geometric Schema, Fourth International Conference on Space Structures, University of Surrey, Guildford, Sept. 1993, 1138–47; PDF 10 at http://www.rmeurant.com/its/papers/polygon-1.html

12. R.C. Meurant, The Myth of Perfection of the Platonic Solids, People and Physical Environment Research PAPER Conference on Myth Architecture History Writing, University of Auckland, New Zealand, July 1991. PDF 07 at http://www.rmeurant.com/its/papers/polygon-1.html

***